Peer Reviewed

Effect of Substrate and Its Shape on in-Flight Particle Characteristics in Suspension Plasma Spraying

K. Pourang, C. Moreau, and A. Dolatabadi

Obtaining a uniform coating on curved mechanical parts such as gas turbine blades is one of the industrial challenges in suspension plasma spraying. Through a three dimensional numerical analysis, this study is aimed at providing a better understanding of the effect of substrate curvature on in-flight particle temperature, velocity, and trajectory. The high temperature and high velocity plasma flow is simulated inside the plasma torch using a uniform volumetric heat source in the energy equation. The suspension of yttria-stabilized zirconia particles is molded as a multicomponent droplet while catastrophic breakup regime is considered for simulating the secondary break up when the suspension interacts with the plasma flow. A two-way coupled Eulerian-Lagrangian approach along with a stochastic discrete model was used to track the particle trajectory. Particle size distribution in the vicinity of the substrate at different stand-off distances has been investigated. The results show that sub-micron particles obtain higher velocity and temperature compared to the larger particles. However, due to the small Stokes number associated with sub-micron particles, they are more sensitive to the change of the gas flow streamlines in the vicinity of a curved substrate.

1. Introduction

In the recent decades, producing nano-structured coatings has been one of the major interesting research subjects due to their notable properties such as better dimensional stability or lower thermal diffusivity compared to conventional ones (Ref 1). One of the challenges in this area was finding a way to inject these nano-sized particles into the gas flow. To address this problem, a new technique called suspension plasma spraying (SPS) is being used. In this technique, suspension of nano-or sub-micron-sized particles in a base fluid (usually ethanol or water) is injected into the plasma plume in a form of liquid jet or train of fragmented droplets (Ref 2). The use of liquid carrier is to provide the required momentum for the small-sized particles to penetrate inside the plasma. However, transport of suspension into plasma flow is a complex phenomenon and there are various parameters that affect the properties of the SPS coatings such as torch operating condition, plasma arc fluctuation, suspension jet/droplets penetration, fragmentation, and evaporation (Ref 3). Moreover, droplet jet velocity and orientation of the injector (angle) are found to be important parameters that affect the heat and momentum transfer in a radial injection SPS (Ref 4). Consequently, coating quality and deposition efficiency depend on some key factors such as particles' velocity, size, and temperature upon impact (Ref 3). Furthermore, it was reported that particles' velocity and temperature are mostly affected by the actual plasma torch conditions and feed stock parameters, respectively (Ref 5). Over the past years alongside the experimental works, numerical study of the plasma spray process has been proven a useful tool to find a path to a better understanding of these complex phenomena that are involved in this deposition process. Most of these studies are based on using a Lagrangian approach in which a large number of the injected particles that can change momentum, mass, and energy with the flow are tracked.

Remesh et al. (Ref 6) studied the behavior of multi-sized particles injected in plasma plume. In this study, the authors modeled the arc heating by adding an energy source in the energy equation. Meillot et al. (Ref 7) proposed a time-dependent moving energy volume to take into account the plasma arc movement within the torch. Throughout the literature, it has been shown that fragmentation of liquid feed stock is one of the major parameters that control the size of droplets. Shan et al. (Ref 8) simulated the plasma flow alongside droplet collision and break up by utilizing Re-Normalization Group (RNG) k-ε, with Taylor Analogy Breakup (TAB) model. They reported that both droplet collision and break up

---

K. Pourang, C. Moreau, and **A. Dolatabadi**, Department of Mechanical and Industrial Engineering, Concordia University, Montreal, QC Canada. Contact e-mail: ali.dolatabadi@concordia.ca.

should be considered in the simulation. By injecting different size water droplets into the transient plasma, Marchand et al. (Ref 9) investigated the evolution of droplets' Weber number along with their trajectories. The author's work showed a need for a break-up model which can adapt itself to these changes. Therefore, due to this level of complexity in liquid atomization, there has been an increasing interest in simulating liquid atomization in plasma spraying by using more accurate approaches such as volume of fluid (VOF) technique. The advantage of this technique is that it can solve the fragmentation of liquid in small scales rather than using empirical correlations. An example of this approach is the work of Meillot et al. (Ref 10) in which fragmentation of the liquid feedstock injected in steady plasma was simulated in a 4 mm × 2.56 mm × 1 mm zone in front of the nozzle exit. Jabbari et al. (Ref 11) developed a model to investigate the suspension atomization, evaporation, and break up within an argon plasma flow. In this study, plasma flow exiting the torch was modeled by assuming a parabolic velocity and constant temperature profiles.

It is a known fact that the presence of a substrate affects the fluid flow and particles' trajectories that are injected into the plasma flow especially in the vicinity of the substrate. Thus, the effect of inclusion of a substrate on the plasma flow and the particles' trajectories has been investigated both experimentally and numerically. Kang et al. (Ref 12) studied the effect of adding a flat substrate on the behavior of injected inflight particles near the substrate. They showed that the zone influenced by the substrate is rather small and particle parameters are mainly unaffected and similar to those of the free jet case for particle sizes ranging from 22 to 125 μm. In another study with the same conditions (Ref 13), the authors investigated the effect of inclusion of a curved substrate; they suggested that there is a threshold for particle diameter (10 μm) above which particles are unsusceptible to the flow. Recently, the effect of adding a flat substrate on an argon plasma flow with same conditions and assumptions in Ref 11 was investigated in SPS process by Jadidi et al. (Ref 14). They analyzed the effect of standoff distance on the impact condition of submicron particles and concluded that due to the stagnation region formed near a flat plate many small size particles would get diverted especially for

shorter standoff distances. The aim of the current study is to address the challenges to obtain a desired SPS coating on curved parts such as airfoils compared to flat substrates. Although the aim of this paper is to investigate coating on curved parts, simulations on flat substrate and free jet case were also carried out and included so one could compare the results. This is done through a numerical analysis of suspension penetration, evaporation, and finally particle transport all the way to the flat and the curved substrates located at various stand-off distances.

2. Geometry and Operation Conditions

Throughout this study, the term droplets are used for the suspension droplets and the term particles means the zirconia particles either in solid or molten state. Figure 1 shows a 3D view of the plasma torch, suspension injection, and substrates configuration. The simulated plasma torch is a 3 MB Oerlikon-Metco gun with 20 mm long anode and 6 mm diameter exit nozzle. The flat substrate has dimensions of $25 \times 25 \times 2$ mm^3 whereas an 80 mm long cylinder with a diameter of 25 mm is used to represent the curved substrate. The operating conditions for plasma and suspension flow are summarized in Table 1. These conditions (Table 1) are chosen so this work could be compared with the ongoing experiments as future work. Suspension used in this study contains zirconia particles (10 wt.%) and ethanol as the solvent. The thermo-physical properties of zirconia and ethanol used in this study are presented in Table 2 (Ref 12, 16).

Table 1 Suspension plasma spray operating conditions

Plasma gun operating conditions

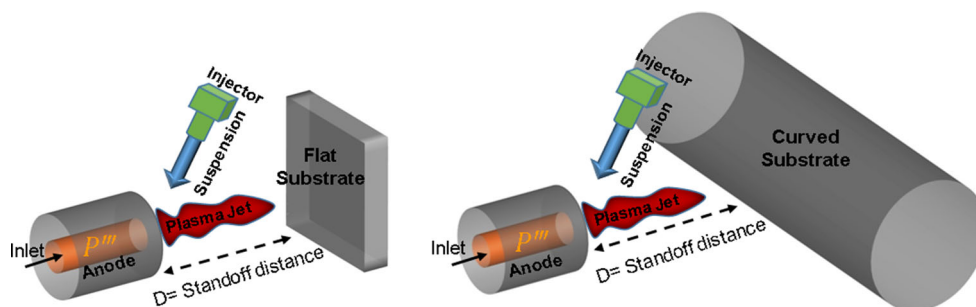|	
Nozzle diameter, mm	6
Arc current, A	500
Arc voltage, V	60
Thermal efficiency, %	60
Ar_H$_2$ mass flow rate, g/s	1.48

Fig. 1 The schematic of plasma flow and substrate configuration

3. Mathematical Modeling

An example of computational domain for the case of curved substrate is shown in Fig. 2, It contains 800,000 hexahedral cells which are locally refined in the plasma core area to capture the large plasma temperature and velocity gradients. At the inlet, boundary condition is set as mass flow rate. In addition, turbulence at the inlet is incorporated by turbulence intensity (4.5%) and hydraulic diameter. The temperature at the torch walls is set at 300 K due to the effect of water cooling while substrate temperature is fixed at 700 K (Ref 14). For the side and outlet boundaries, pressure inlet and pressure outlet conditions are used.

A two-way coupled Eulerian-Lagrangian approach is applied in this study. The governing equations (continuity, momentum, energy and species transport) were solved by means of ANSYS-Fluent v14.5 commercial software package. This is done by using a pressure based solver and the SIMPLE algorithm for pressure velocity coupling. Reynolds Stress Model (RSM) is used for modeling turbulence due to its potential to take into account streamline curvature, swirl and rotation (Ref 16). A steady state solution is obtained to model the plasma flow where Ar_H_2 (10%) is considered as the plasma gas. The thermodynamic and transport properties of Ar_H_2 mixture are obtained from (Ref 15). In this study, plasma is considered as a Newtonian compressible chemically inert gas and it is assumed to be in local thermal equilibrium condition. A constant volumetric heat source located inside the torch is added in the energy equation to account for the plasma heat generation. This energy source is calculated from,

$$P''' = \frac{\eta_t EI}{V},$$ (Eq 1)

where E, I, V, η_t are arc voltage, current, anode volume, and thermal efficiency, respectively. Capturing the velocity and
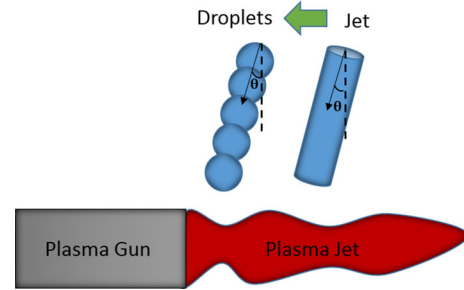
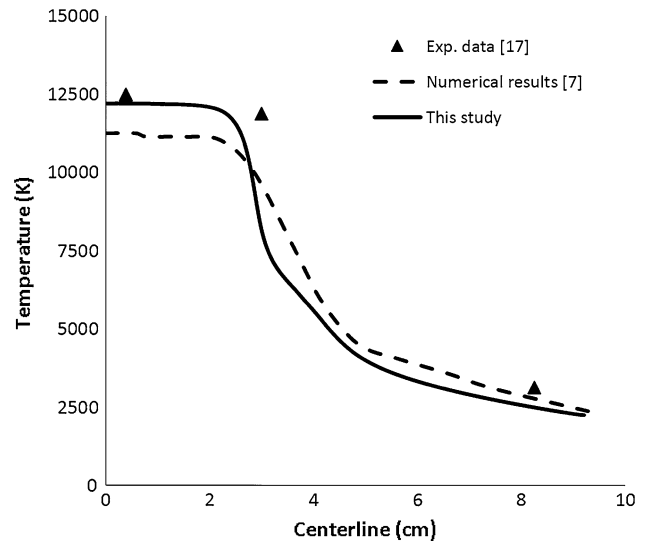**Fig. 3** Schematic suspension injection into the plasma plume

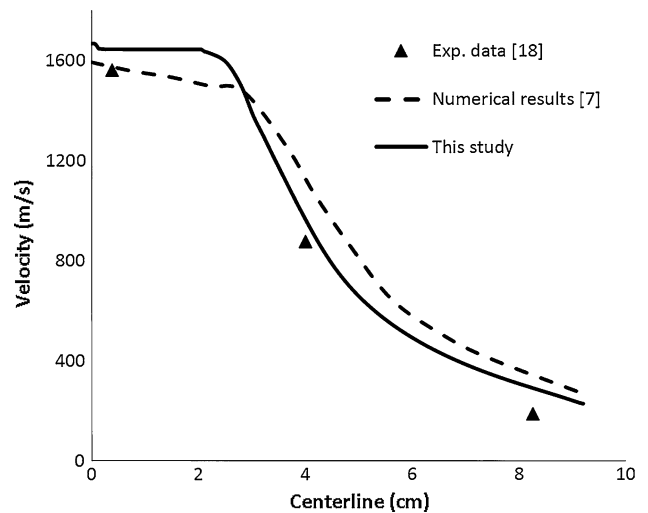**Fig. 4** Plasma temperature evolution along the centerline

Fig. 5 Plasma axial velocity along the centerline

Table 2 Materials thermo-physical properties

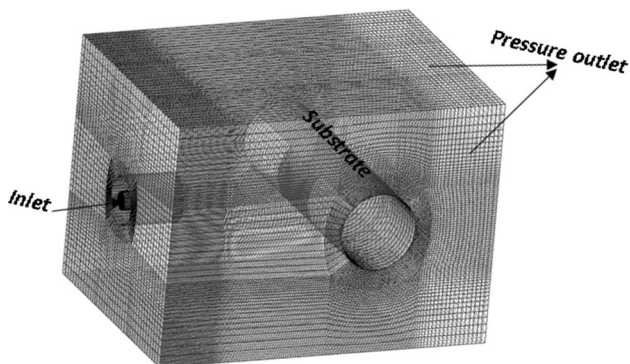| Property	Units	Molten zirconia	Ethanol
Density	kg/m³	5680	789
Specific heat	J/kg K	1387	2470
Surface tension	N/m	1.5	0.0223
Melting point	K	2988	…
Boiling point	K	5273	351
Viscosity	m²/s	6.5×10^{-6}	1.2×10^{-3}
Melting latent heat	J/kg	7.7×10^{3}	…
Boiling latent heat	J/kg	9×10^{6}	855,237

Fig. 2 Computational domain

thermal boundary layers especially on the substrate is highly important in this study for the prediction of particle conditions upon impact. This is achieved by using semi-empirical formulas called "wall functions". This approach is explained in detail in (Ref 16). Modeling suspension is achieved using a similar approach to the one described in detail in (Ref 11); the suspension is modeled as a multi-component droplet that carries properties of yttria-stabilized zirconia (10 wt.%) particle and ethanol as the solvent. These droplets undergo break up and evaporation and each newly generated droplet has the same concentration as far as the break up is dominant (Ref 2, 11). In order to model the primary atomization, here instead of injecting suspension in the form of a continuous jet, droplets with a uniform size of 150 µm and velocity of 30 m/s

(same as the continuous jet) are injected radially with a backward angle of 14° with respect to the normal plane to the plasma plume (θ as shown in Fig. 1, 3). Droplets are injected with a sequence of 3.2 µs to provide the same dimensionless numbers (Weber, Reynolds) as in the uniform jet and the same suspension mass flow rate presented in Table 1. Due to the existence of catastrophic break up inside the plasma plume (Ref 2), KHRT break-up model is used which combines Kelvin-Helmholtz waves with Rayleigh-Taylor instabilities. O'Rourke's model (Ref 16) is applied to simulate the droplet collision in this study. Particle dynamic equation can be written by the use of force balance including inertia and drag forces. The drag coefficients are calculated from the following correlation,
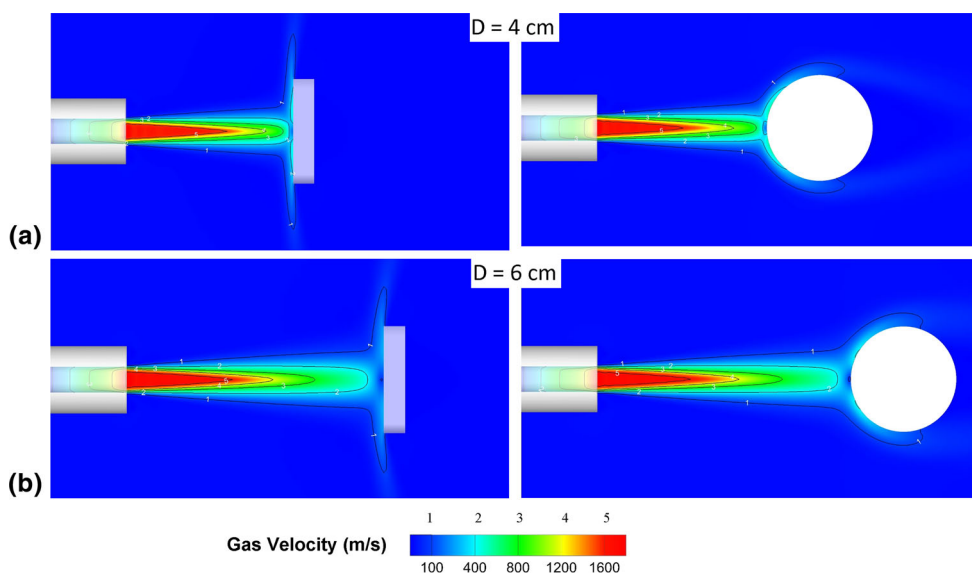

Fig. 6 Plasma velocity contours for (a) flat and (b) curved substrates at standoff distances of $D = 4$ cm and $D = 6$ cm (Color figure online)
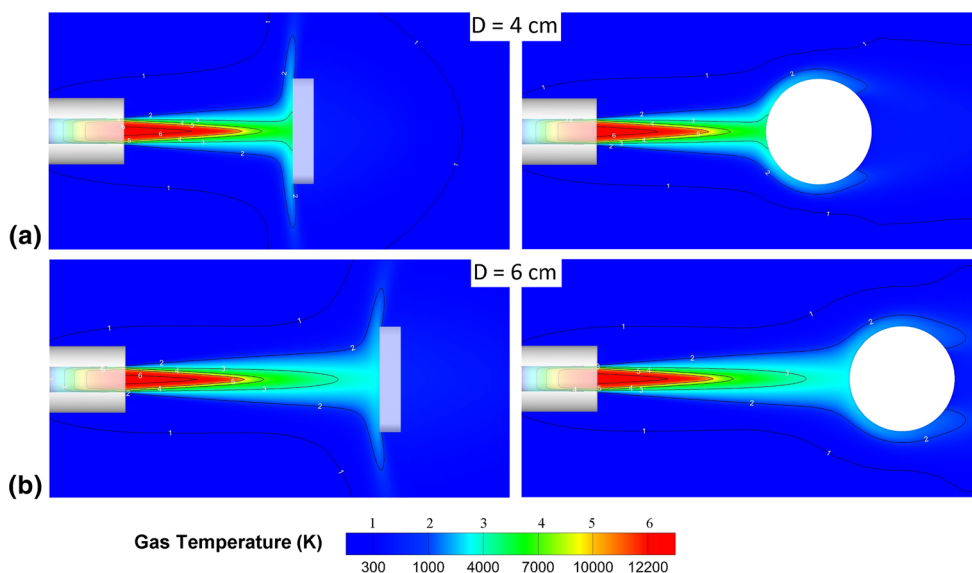

Fig. 7 Plasma temperature contours for (a) flat and (b) curved substrates at standoff distances of $D = 4$ cm and $D = 6$ cm (Color figure online)
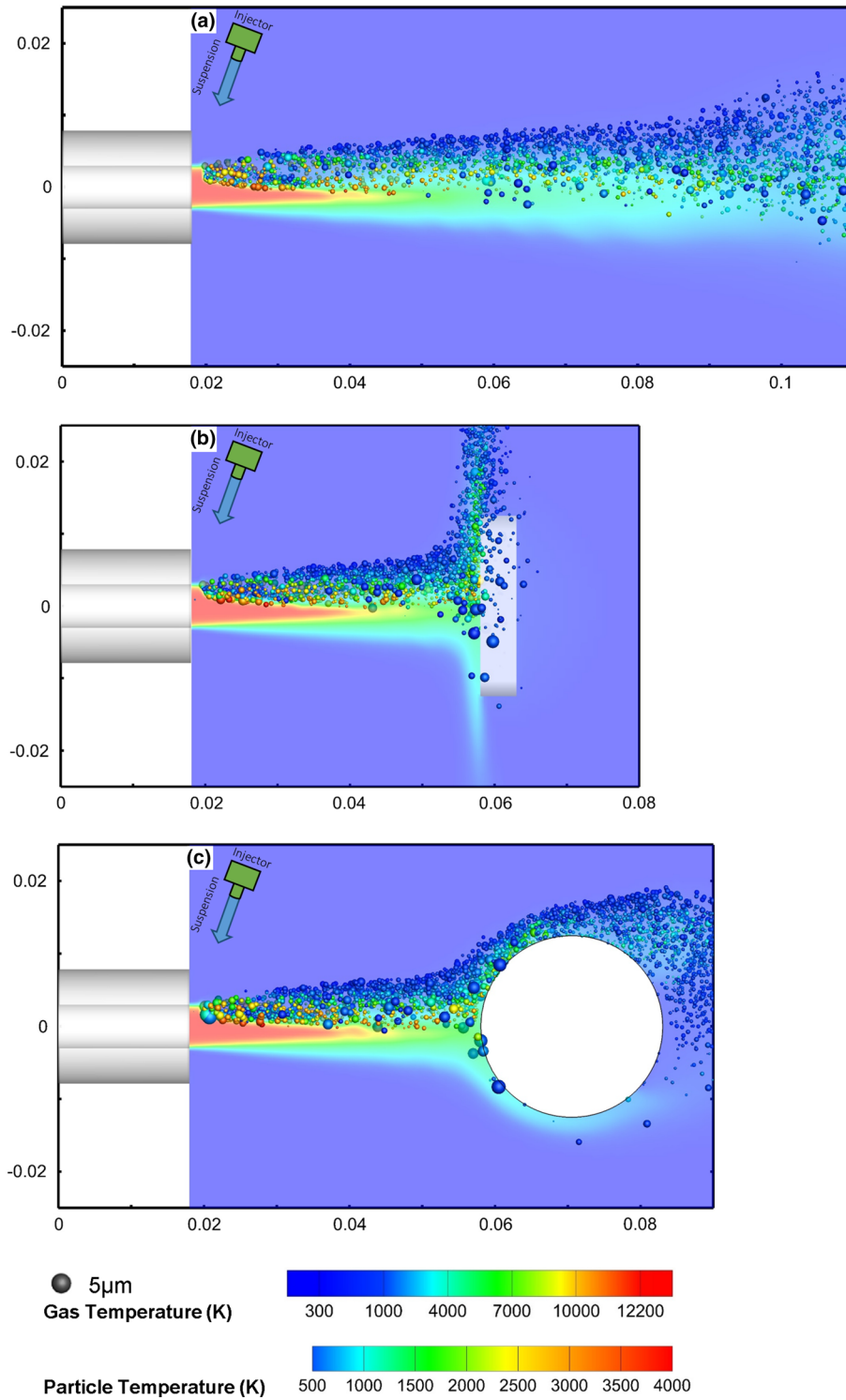
Fig. 8 Plasma temperature contours with particle temperature injected in (a) free jet, (b) case with inclusion of flat substrate and (c) case with inclusion of curved substrate located at $D = 4$ cm (dimensions are in meters) (Color figure online)

$$C_{\mathrm{D}} = a_1 + \frac{a_2}{Re} + \frac{a_3}{Re^2}, \qquad (\text{Eq } 2)$$

where Re is the Reynolds number while a_1, a_2 and a_3 are constants (Ref 16). A stochastic approach is used to take into account the effect of turbulence on particle dispersion. Lumped capacity method is used for analyzing the heat transfer due to the rather low Biot number associated with the suspension droplets and particles. Heat of fusion of zirconia particles is embedded in the temperature-de-
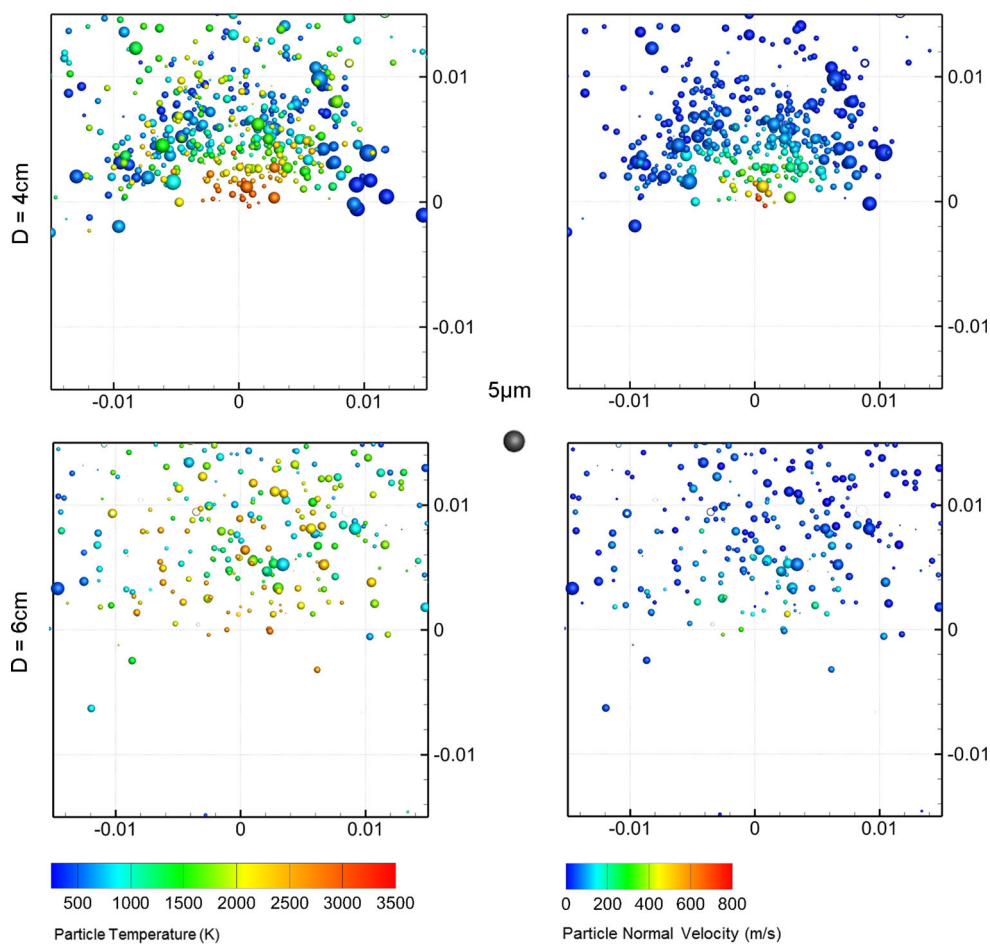
Fig. 9 Landing location, particle temperature, size and velocity distributions on the flat substrate for standoff distances of 4 and 6 cm (dimensions are in meters) (Color figure online)

pendent Cp in a similar way done in (Ref 11) to model the particles' melting. Lewis number is assumed to be one for calculation of the diffusion coefficients in this study. Both Nusselt and Sherwood numbers are calculated from Ranz-Marshal correlations (Ref 16) for finding the convection heat and mass transfer coefficients.

4. Results and Discussions

The focus of this study is to investigate the effect of the substrate and its shape on deposition of particles. To do so, in the first step, a free jet case without the inclusion of a substrate is modeled and then results were compared with other studies for validation purposes. Then, the effect of obstruction of a flat substrate on plasma gas flow and in-flight particle trajectories is studied. Furthermore, the effect of substrate curvature is investigated by obstruction of a cylinder which will be referred to as the curved substrate in this work. Finally, effect of changing the suspension momentum on inflight particles characteristics is discussed in this paper.

4.1 Free Jet

In order to validate the plasma flow model, a free jet model without the inclusion of substrate was created first. Then, the result of this study is compared with the numerical study in Ref 7 which is referred to as the stationary case and experimental work of Ref 17 and 18. Figure 4 and 5 show the evolution of temperature and velocity of the plasma gas along the torch axis which is in good agreement with numerical and experimental works mentioned above. In order to examine the sensibility of the solution to the grid size, a fine mesh in which volume of each cell is reduced by a factor of 8 is generated. The largest difference between the solutions of these two grids is observed to be less than 4% in the worst case condition. Therefore, because of the large computational time and cost related to the fine grid, the coarse grid is used in this study.

5. Effect of Placing a Substrate

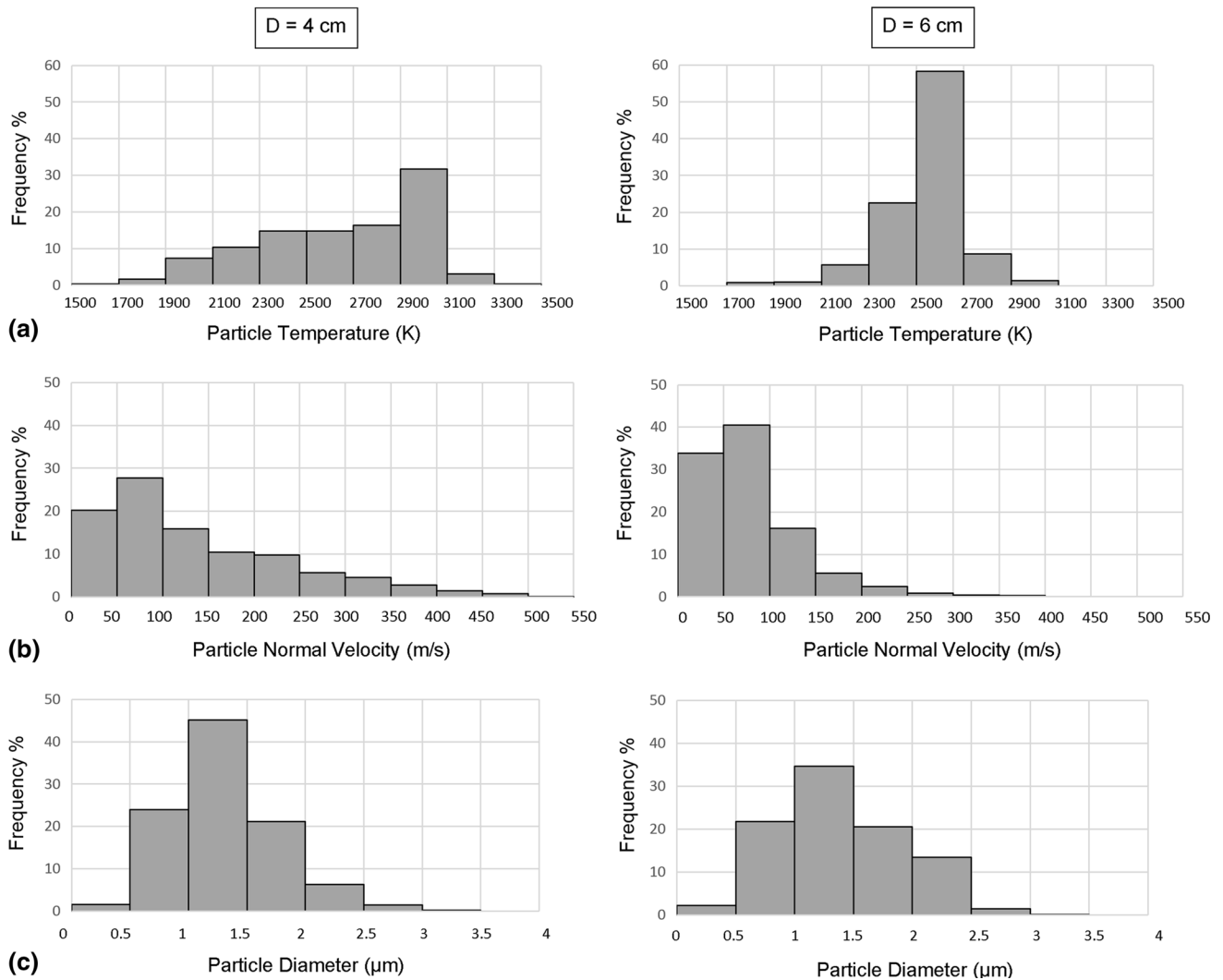The effects of presence of the flat and the curved substrates were studied at different standoff distances of 4 and

Fig. 10 Quantitative analysis on the (a) temperature, (b) velocity and (c) diameter of spray particles landing on the surface of a flat substrate at standoff distances of 4 and 6 cm

6 cm ($D = 4$, $D = 6$). Figure 6 shows that as the flow approaches the substrates (both flat and curved), its axial velocity decreases rapidly and forms a region called stagnation region. Eventually the fluid is brought to a complete stop at the stagnation region and leads to a pressure increase in this region. Then, plasma gas enters the wall jet region after turning and moves in radial direction and forms a wall jet. The pressure decreases as the flow accelerates from the stagnation point parallel to the flat substrate or around the cylinder. Additionally, it can be seen from Fig. 6 that by increasing the standoff distance to $D = 6$ cm in both cases due to deceleration of the axial flow, a weaker stagnation flow forms in front of the substrates. The evolution of plasma temperature for these two substrates at two different standoff distances is also evident in Fig. 7.

Calculation of Weber number based on the injector diameter (150 µm) and the flow parameters in this work, showed a variation range between 500 at centerline to 250
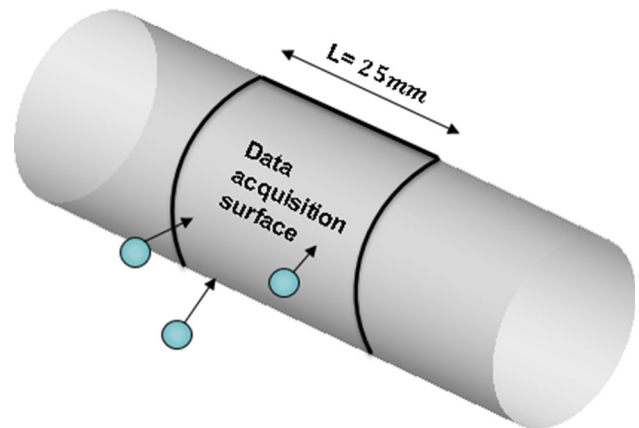

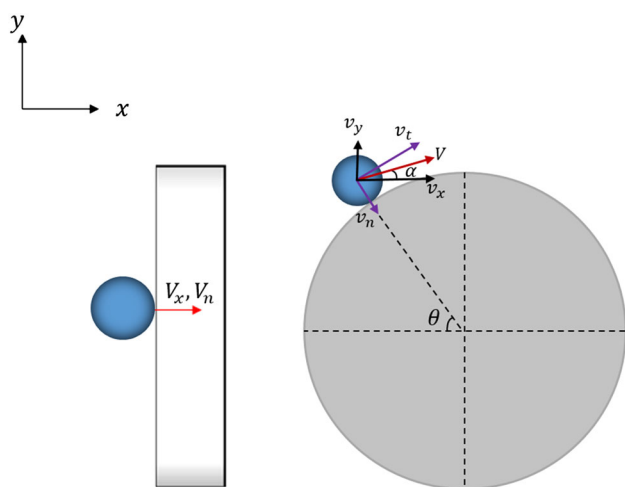**Fig. 11** Acquisition data region on the curved substrate

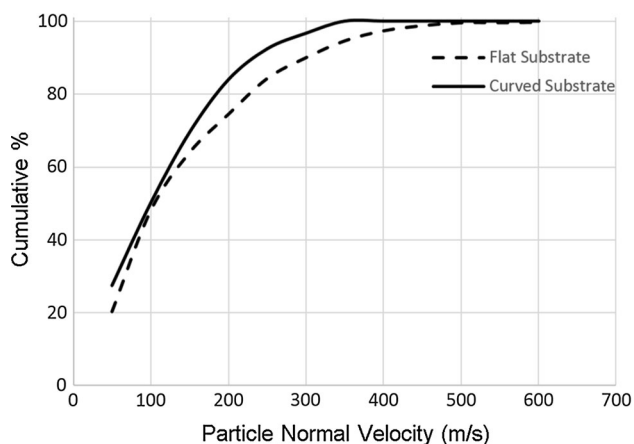**Fig. 12** Particle normal velocity on flat and curved substrates

Fig. 13 Cumulative particle normal velocity on flat and curved substrates at $D = 4$ cm

at 3 mm above it. This justifies the use of the KHRT break-up model for this study. The next set of results represents the particle trajectories and their temperature distributions in space as they are injected in three different cases: (1) in a free jet, (2) the inclusion of flat substrate, and (3) with the inclusion of the curved one. It should be noted that here results showing the particles/droplets trajectories in the following figures are filtered so that only zirconia particles are shown. These distributions are accompanied by the plasma gas temperature contour to examine the interaction between plasma gas and injected droplets at the same time. Results in these three different cases are shown in Fig. 8. Figure 8(a) shows the suspension injection into a free jet and inflight particles trajectories that are traveling along the plasma gas without feeling any disturbance caused by inclusion of substrate. It can be observed that the fine particles (~0.5 to 2 μm) that are located near the torch centerline gained higher temperature comparing to the rest of the particles that are traveling in the fringes of the plasma plume. Particles that

are traveling in the fringes of the plasma stay in larger sizes compared to the rest. The effect of insertion of a flat and a curved substrate on inflight particles are shown in Fig. 8(b) and (c), respectively. It should be noted that the trajectories of the smaller sized particles (below 2 μm) are more influenced by the change of the flow pattern caused by the insertion of substrate as it can also be seen in Fig. 8(b) and (c).

These small particles also gain higher temperature compared to the large ones. It is also noted that most particles pass over the upper part of the flat and curved substrates indicating that the suspension injection conditions are not optimal. Due to the high melting point of zirconia particles (around 3000 K) many of them do not become fully molten before striking on the substrate (see Fig. 8b, c) which can result in rather small deposition efficiency. Figure 9 shows a cross-sectional view of the particle landing location, temperature, normal velocity, and a size scale in a $25 \times 25 \times 0.2$ mm^3 rectangular box located in front of the flat substrate at 4 and 6 cm standoff distances. By inspecting the results at $D = 4$ cm, it is evident that high temperature (molten) and high velocity particles are traveling close to the centerline. These particles cool down and decelerate by increasing the standoff distance ($D = 6$).

Particles with relatively low temperature and velocity correspond to the suspension drops that do not penetrate efficiently into the plasma plume and travel in low-temperature zones that surround the plasma plume. Consequently, these particles may generate important defects in the produced coatings by SPS. The deviation of particles from the center is much more evident for the case at 6 cm standoff distance. Based on the observations above, it can also be expected that denser coatings will be produced at a shorter standoff distance (4 cm) as compared to 6 cm. In order to perform a quantitative analysis on the particle data landing on the surface of the flat substrate, a surface (25 mm × 25 mm) located on the front surface of the flat substrate is chosen. Data corresponding to the particles that reach this surface at the standoff distances of 4 and 6 cm were recorded and illustrated in Fig. 10. Figure 10(a) shows that more than 30% of the incident particles on the flat substrate are in a molten state. The high melting point of zirconia and evaporation of zirconia particles are examples among numerous factors that have influence on the quantity of molten particles. As it can be seen from Fig. 10(a), the particles temperature dropped below the melting point by increasing the standoff distance to $D = 6$ cm. Deviation of particles from the centerline along with rapid decrease in plasma gas temperature at longer stand-off distances could explain the presence of a high number of non-molten particles in the case of $D = 6$. Figure 10(b) illustrates the particles normal velocity distributions at both spray distances. As shown in this figure, the particles will impact the flat substrate with higher normal velocity at $D = 4$ cm compared to $D = 6$ cm. This is expected since the plasma axial velocity decreases along the centerline as standoff distance increases. Consequently, particles would decelerate by increasing the
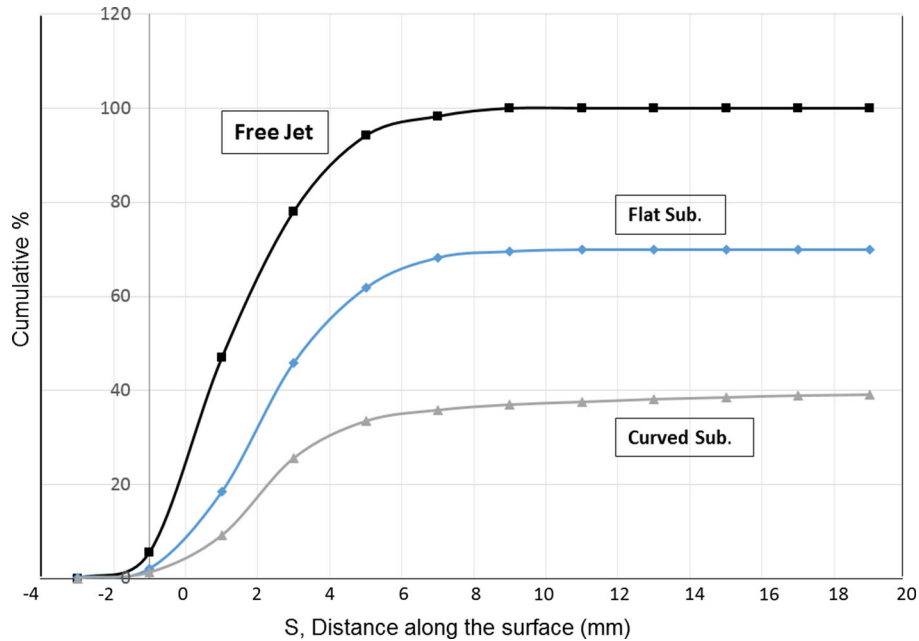
Fig. 14 Distribution of the particle landing location in case of free jet, curved substrate, and flat substrate at $D = 4$ cm as a function of distance along the surface, S

standoff distance and hit the surface with still lower normal velocity. Figure 10(c) shows that the most probable particle diameter range is 1 to 1.5 μm for incident particles at $D = 4$ cm. However at $D = 6$ cm, the diameter distribution shifts slightly to higher values. As mentioned above, particles at longer standoff distances acquire lower normal velocity, thus smaller particles tend to deflect more and results in a bigger size distribution at longer standoff distances. Therefore, from the discussion above it can be concluded that particles at 4 cm standoff distance contribute more in creating a uniform coating by having higher temperature and velocity compared to the case at a standoff distance of $D = 6$ cm.

6. Effect of Substrate Shape

In the next step for the curved substrate located at a standoff distance of 4 cm, a curved surface with a length L covering the front of the cylinder (see Fig. 11) is chosen to record the data associated with particles landing on the substrate. Similar to the case of flat substrate, quantitative analyses on landed particles on the curved substrate are performed and results are compared with data for the flat substrate located at the same standoff distance. By inspecting the number of the incident particles in these two cases (flat and curved substrates) during a fixed time interval ($\Delta t = 1$ ms), it is interestingly observed that particles hit the flat substrate nearly 2.2 times more frequently as compared to the curved one. Based on this observation, a parameter called "Catch Rate" is defined by Eq 3.

$$\text{Catch rate } (\%) = \frac{\text{mass of landed particles in } \Delta t}{\text{mass of injected particles in } \Delta t} \times 100$$

(Eq 3)

The observed catch rate on the flat substrate is 23% while it decreases to 11% on the curved substrate. This significant catch rate decrease on the curved substrate would result in a much lower deposition on curved substrates. It is known that the normal component of the particle impact velocity has a major influence on the deposition of the particles landing on a flat substrate. Using the same analogy, the distribution of the particle normal velocity components, V_n, is investigated in this study for the curved substrate. This is further explained with the schematic view shown in Fig. 12.

The cumulative particles normal velocity distributions for the two different substrates at $D = 4$ cm are illustrated in Fig. 13. This figure indicates that particles tend to hit the flat substrate with a slightly higher normal velocity compared to the curved substrate. Furthermore, the distribution of the particle landing location on flat and curved substrates at $D = 4$ cm along the distance S (as shown Fig. 12) was calculated. Then these results are compared to the results of the free jet case in which particles are going through an imaginary plane locating at same distance and with same dimensions as the flat substrate (25×25 mm^2). These results are shown in Fig. 14 as a function of cumulative percentage which is calculated based on the number of the particles. It should be noted that in Fig. 14, the number of landing particles on the two substrates is normalized based on the number of particles
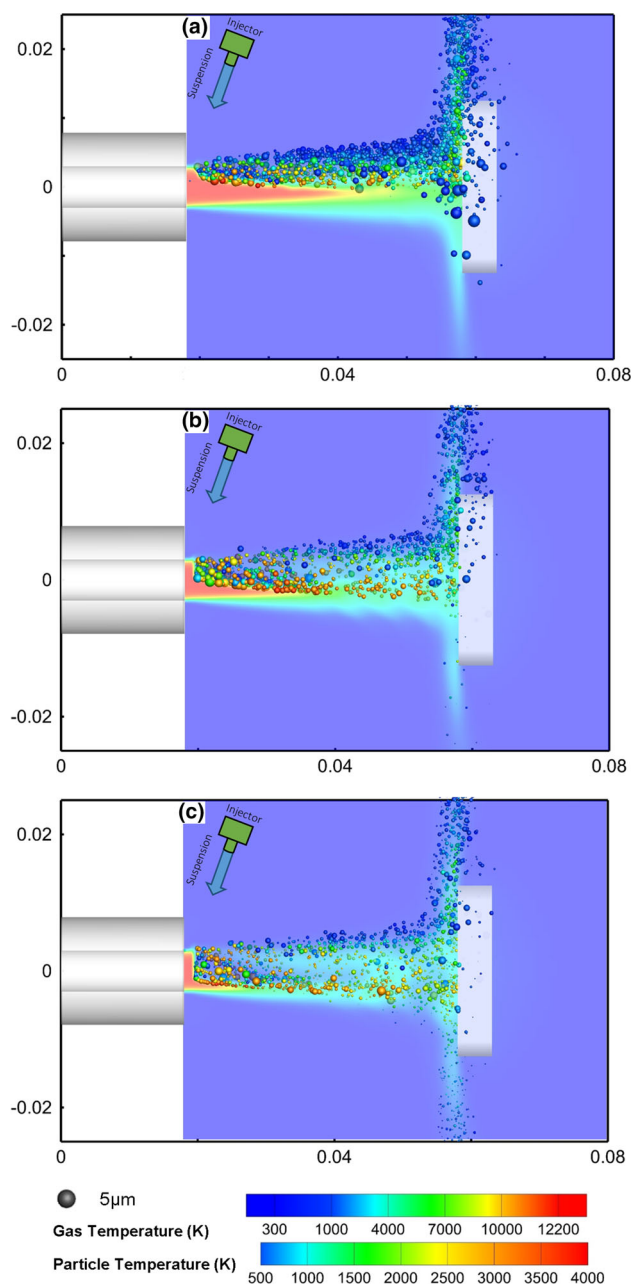
Fig. 15 Plasma temperature contours with temperature of the injected particles in case of flat substrate with suspension droplet velocity of (a) 30, (b) 37.5 and (c) 45 m/s located at $D = 4$ cm (dimensions are in meters) (Color figure online)

Table 3 Suspension velocity (a) 30, (b) 37.5, and (c) 45 m/s

Case	Suspension velocity, m/s
a	30
b	37.5
c	45

passing through the imaginary surface in the free jet case. As shown in Fig. 14, in the absence of a substrate (i.e., free jet case) more than 40% of inflight particles pass the imaginary plane at S between 0 and 2 mm. Adding a flat substrate scatters these inflight particles from the center-line, shifts the peak of the distribution to S values of 2-4 mm and induces a wider distribution in S direction of the particle landing location. In the case of the curved substrate, most of the inflight particles hit the curved sub-strate at locations of 2-4 mm ($10° < \theta < 20°$) and, as we move along the surface (in the S direction), the number of landed particles decreases rapidly compared to flat sub-strate case. Comparing the number of the landed particles on the curved substrate with the other cases in Fig. 14, it is evident that a lower deposition rate is going to be obtained on the curved substrate compared to the flat one. The dif-ference between Fig. 14 and the calculated catch rates arises from the fact that the definition of the catch rate is based on the mass of the particles while in Fig. 14 values are based on the quantity of them. It is important to note that although the catch rate of the cylinder is half of the flat substrate, the formation of a weaker stagnation pressure on the curved substrate will result in higher impact particle velocity specifically near the centerline.

7. Effect of Suspension Momentum

By inspecting Fig. 8, it was concluded that suspension injection is not optimal. In order to reach an optimal condition for the suspension injection, the effect of changing the suspension momentum on in-flight particles' trajectories and properties in the case of a flat substrate located at a 4-cm standoff is investigated in this sec-tion. Figure 15 shows the effect of increasing the suspen-sion momentum by increasing the droplets velocity by 25 and 50% for cases (b) and (c) as shown in Table 3, respectively. By inspecting Fig. 15, it is evident that, in cases (b) and (c), increasing the momentum has increased the penetration depth of the injected suspension droplets into the plasma. Furthermore, compared to case (a), case (b) shows a higher penetration depth and, as a conse-quence of a more severe fragmentation of the droplets, smaller particle size distributions are obtained. Another important observation from Fig. 15(b) is that the quantity of cold particles, which correspond to those that did not penetrate inside the plasma gas, has significantly de-creased and overall a higher particle temperature distri-bution is obtained. In addition, since the particles are closer to the centerline in case (b), they will acquire higher normal velocities compared to case (a). Case (c) shows the example of an excessive increase in suspension momen-tum. From Fig. 15, it is apparent that too much suspension penetration into the plume has significantly cooled down and disturbed the entire plasma high temperature core. From the above discussion, it can be concluded that there

is an optimum value for increasing the suspension momentum and above that, suspension cools down and disturb the entire plasma core leading to low particle temperature and velocity distribution and consequently an expected poor coating quality.

8. Conclusion

The main goal of this paper is to investigate the effect of substrate shape on the inflight particles trajectories and characteristics especially at the vicinity of the substrate. Results of landing particles on the curved substrate are then compared with the results for the flat substrate and the free jet case. This is done through a 3D numerical study by means of a two-way coupled Eulerian-Lagrangian approach along with the Reynolds Stress turbulent Model. It was observed that the presence of the substrate and shape of the substrate has no influence on the injection conditions, atomization, and evaporation of the solvent near the nozzle exit. However, the results showed that the substrate shape has a significant influence on the particles trajectory and their normal velocity in the vicinity of the substrate. It was found that, in a fixed time interval, particles hit the flat substrate 2.2 times more often than observed on the curved substrate. Based on this finding, a new parameter called "Catch Rate" was introduced. In addition, the particle landing location as a function of the distance along the surface was calculated and compared for three cases of free jet, flat, and curved substrates. It was observed that most of the particles tend to hit the surface of the cylinder at angles between ($10° < \theta < 20°$) and above this range, particles pass over the curved substrate without striking on it. Furthermore, it was shown that there is an optimum value for suspension momentum. Excessive increase in the suspension momentum was found to disturb the plasma high temperature potential core, resulted in low particle temperature and velocity and consequently led to a poor deposition efficiency. Moreover, by investigating the effect of changing the substrate standoff distance it was observed that a higher deposition is expected in the shorter standoff distance.

Acknowledgment

References

1. P. Fauchais, J.V.R. Heberlein, and M.I. Boulos, *Thermal Spray Fundamentals*, Springer, New York, 2014
2. J. Fazilleau, C. Delbos, V. Rat, J.F. Coudert, P. Fauchais, and B. Pateyron, Phenomena Involved in Suspension Plasma Spraying Part 1: Suspension Injection and Behavior, *Plasma Chem. Plasma Process.*, 2006, **26**(4), p 371-391
3. P. Fauchais, R. Etchart-Salas, V. Rat, J.F. Coudert, N. Caron, and K. Wittmann-Ténèze, Parameters Controlling Liquid Plasma Spraying: Solutions, Sols, or Suspensions, *J. Therm. Spray Technol.*, 2008, **17**(1), p 31-59
4. J.O. Berghaus, S. Bouaricha, J.G. Legoux, and C. Moreau, Injection Conditions and In-Flight Particle States in Suspension Plasma Spraying of Alumina and Zirconia Nano-ceramics, *Proceedings of the International Thermal Spray Conference* (Basel, Switzerland). CD-ROM, 2005, p. 512-518
5. F. Tarasi, M. Medraj, A. Dolatabadi, J.O. Berghaus, and C. Moreau, Effective Parameters in Axial Injection Suspension Plasma Spray Process of Alumina-Zirconia Ceramics, *Therm. Spray Technol.*, 2008, **17**(5-6), p 685-691
6. K. Remesh, S.C.M. Yu, H.W. Ng, and C.C. Berndt, Computational Study and Experimental Comparison of the In-Flight Particle Behavior for an External Injection Plasma Spray Process, *J. Therm. Spray Technol.*, 2003, **12**(4), p 508-522
7. E. Meillot, D. Guenadou, and C. Bourgeois, Three-Dimension and Transient DC Plasma Flow Modeling, *Plasma Chem. Plasma Process.*, 2008, **28**(1), p 69-84
8. Y. Shan, T.W. Coyle, and J. Mostaghimi, Numerical Simulation of Droplet Breakup and Collision in the Solution Precursor Plasma Spraying, *J. Therm. Spray Technol.*, 2007, **16**(5-6), p 698-704
9. C. Marchand, A. Vardelle, G. Mariaux, and P. Lefort, Modelling of the Plasma Spray Process with Liquid Feedstock Injection, *Surf. Coat. Technol.*, 2008, **202**(18), p 4458-4464
10. E. Meillot, D. Damiani, S. Vincent, C. Caruyer, and J.P. Caltagirone, Analysis by Modeling of Plasma Flow Interactions with Liquid Injection, *Surf. Coat. Technol.*, 2013, **220**, p 149-156
11. F. Jabbari, M. Jadidi, R. Wuthrich, and A. Dolatabadi, A Numerical Study of Suspension Injection in Plasma-Spraying Process, *J. Therm. Spray Technol.*, 2014, **23**(1-2), p 3-13
12. C.W. Kang, H.W. Ng, and S.C.M. Yu, Comparative Study of Plasma Spray Flow Fields and Particle Behavior Near to Flat Inclined Substrates, *Plasma Chem. Plasma Process.*, 2006, **26**(2), p 149-175
13. T. Ba, C.W. Kang, and H.W. Ng, Numerical Study of the Plasma Flow Field and Particle In-flight Behavior with the Obstruction of a Curved Substrate, *J. Therm. Spray Technol.*, 2009, **18**(5-6), p 858-874
14. M. Jadidi, M. Mousavi, S. Moghtadernejad, and A. Dolatabadi, A Three-Dimensional Analysis of the Suspension Plasma Spray Impinging on a Flat Substrate, *J. Therm. Spray Technol.*, 2015, **24**(1-2), p 11-23
15. M.I. Boulos, P. Fauchais, and E. Pfender, *Thermal Plasma: Fundamentals and Application*, Vol 1, Plenum Press, New York, 1994
16. ANSYS Inc., ANSYS FLUENT Theory Guide (USA, 2011)
17. M.P. Planche, Experimental Study of Fluctuating Plasma Jets. Ph.D. Thesis, University of Limoges, France, 1995
18. O. Betoule, Relationships Between the Distributions of Particle Velocity and Temperature and Coating Properties. Ph.D. Thesis, University of Limoges, France, 1994